ARMA 24–1048

Rockfall Barrier Testing in an Open Pit Mine: Comparing Empirical and Modeled Rockfall Dynamics

McNabb, J.C.
University of Arizona Geotechnical Center of Excellence, Tucson, Arizona, U.S.A.
Meyer, B.J.; Potter, J.J.
University of Arizona Geotechnical Center of Excellence, Tucson, Arizona, U.S.A.
Warren, S.N.
National Institute for Occupational Safety and Health, Spokane, WA, U.S.A.
Wagner, D.A.
Geobrugg North America LLC, Algodones, NM, U.S.A.

ABSTRACT: Rockfalls pose severe hazards to miners and infrastructure in open pit mines, and rockfall barrier systems are an increasingly common method for mitigating this hazard. Extensive testing to understand rockfall kinetics and barrier efficacy has been performed in controlled settings and natural environments, but rarely in open pit mining environments. This study is part of a collaboration with the National Institute for Occupational Safety and Health, Geobrugg, and the University of Arizona's Geotechnical Center of Excellence, in which controlled rockfall tests were conducted using synthetic concrete rocks on an open pit highwall with a prototype mobile rockfall barrier system. A solitary rockfall that impacted the barrier with significant force was analyzed to determine the kinetics and kinematics of its fall trajectory leading to the barrier strike. These results are then compared to a best-fit 2D rockfall simulation, showing a close match at the moment of impact into the barrier. Lastly, the effects of highwall bench configuration on the test rock trajectory are assessed, which suggest that minor catch bench loss likely resulted in the test rock attaining dangerously high velocity and lateral trajectory, ultimately sending it into the barrier.

1. INTRODUCTION

Engineering advancements in open pit mining and the ever-growing demand for critical minerals have led to increasingly large open pits, characterized by highwalls thousands of feet tall. This expansion necessitates robust slope monitoring techniques to ensure the safe execution of mining operations. Significant improvements in slope monitoring techniques have enabled a step change in miner safety that allows mining activities to proceed concurrently with active slope movements, provided that critical thresholds are not exceeded (e.g. Carlà et al., 2017; Farina et al., 2013). However, in contrast to the notable progress in monitoring for movements from inches per day to inches per year, monitoring of rapid movement due to rockfall in open pit mining has not seen similar advancements to slope monitoring, presenting a significant and inadequately addressed hazard to miners, equipment, and infrastructure. Engineered barriers are often the last line of defense when attempting to mitigate against rockfall, and their efficacy is of critical importance to personnel or infrastructure relying on the barriers for protection. Extensive rockfall barrier testing has been performed on natural slopes (e.g. Jaboyedoff et al., 2005; Sanchez & Caviezel, 2020), man-made fill slopes (e.g. Williams et al., 2020), vertical drop (e.g. Gerber, 2001), or by numerical modelling (e.g. Mentani et al., 2016; Spadari et al., 2012) to test and assess their efficacy. Despite the great need for rockfall protection in open pit mining environments, rockfall testing rarely occurs on open pit mine highwalls where the effects of benched geometries, which are designed to stop falling rock, can be evaluated with respect to rockfall kinetics.

This paper presents preliminary results of a real-world rockfall test in an open pit mine using a synthetic (fiber-reinforced concrete) boulder that impacted a prototype rockfall barrier system. The kinetics of the test rockfall upon impact with the barrier are compared with a best-fit rockfall model, and the kinematics of the rockfall trajectory are evaluated with respect to the achieved highwall configuration.

2. BACKGROUND

This study is part of a collaboration with the National Institute of Occupational Safety and Health (NIOSH), Geobrugg, and the University of Arizona's Geotechnical Center of Excellence (GCE) to analyze the results of real-world rockfall tests within open pit mines. The rockfall tests were designed and implemented by NIOSH as part of their ongoing research titled *Rockfall Catchment Design and Slope Performance Monitoring at Surface Mines and Quarries*, which aims to increase safety in open pit mines and quarries by using empirical rockfall testing data to (1) improve catch bench design criteria and (2) improve slope monitoring guidelines and capabilities (NIOSH, 2023). The GCE became involved in the project in 2021 as part of their ongoing study *Development and Application of Automated Rockfall Recognition using Computer Vision Approaches applied to Thermal Video from Open Pit Mines* (NIOSH contract 75D30122C14875), which aims to develop a commercially viable rockfall monitoring solution using thermal video and an automated rockfall detection algorithm. The GCE benefitted from the NIOSH rockfall tests by collecting thermal video data during the tests, which unlike natural rockfall, can be assessed in greater detail due to the controlled nature of the tests. Similarly, Geobrugg, a provider of protective barrier solutions for rockfall, joined the project to trial a prototype mobile rockfall barrier solution within the controlled environment of the NIOSH rockfall tests.

3. METHODS

3.1. Rockfall Tests

Rockfall testing took place on September 14th of 2023 at an open pit gold mine in Nevada on a section of highwall approximately 116 m (approximately 380 ft) tall. The highwall was composed of four 24.4 m (80 ft) double benches, and one partial bench created by an inclined haul road. The interramp and bench configurations of the test highwall are shown in Table 1. The highwall geology consists of faulted and folded Paleozoic carbonate and clastic sedimentary rocks intruded by a quartz monzonite porphyry of Jurassic age, with small offset (<10 m) normal faulting prevailing in the immediate test area. Figure 1 shows an oblique view of the test highwall from a drone photogrammetry point cloud collected prior to testing.

Table 1. Rockfall test highwall configuration

Total Slope Height (m)	~116
Full Bench Height (m)	24.4
Lowermost Partial Bench Height (m)	16
Number of Catch Benches	4
Interramp Slope Angle (deg)	54

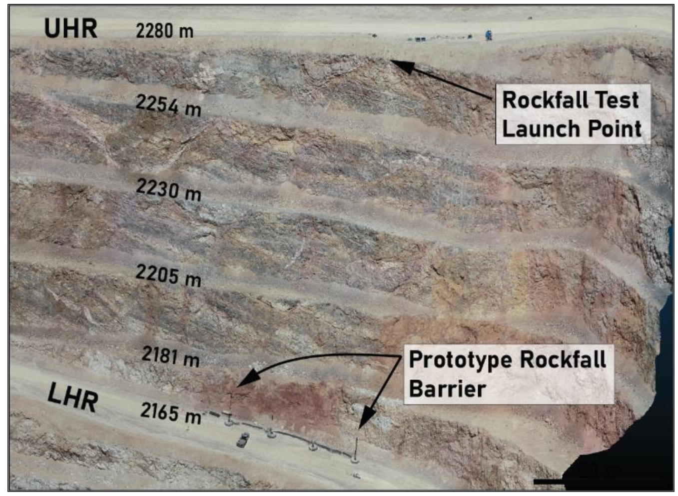

Figure 1. Oblique view of the test highwall from a drone-photogrammetry-derived 3D point cloud.

The tests utilized synthetic 'rocks' made of cast concrete and fiber reinforcement created by the NIOSH team, with various dimensions as shown in Figure 2. The variety in size and dimensions of the synthetic rocks is meant to mimic the natural variety of loose rock that may become rockfall hazards (Warren et al., 2022).

Figure 2. Variety of synthetic rocks created by NIOSH for rockfall testing (from Warren et al., 2022).

Rockfall tests were initiated from the upper haul road (UHR) using a telehandler tractor by loading the rocks onto a wooden pallet, setting the pallet on a flat-top berm on the highwall crest along the UHR, and using another pallet attached to the telehandler forks to push the rocks over the edge. Most rocks were caught by intermediate benches, however several successfully made it to the lower haul road (LHR), impacting the rockfall barrier system described below. Over 300 rocks were sent down the slope during the daylong test, and the NIOSH team plans to analyze the full results of these tests with respect to bench performance. A solitary rhombicuboctahedron-shaped rock measuring 46 cm in diameter and weighing ~172 kg, known here as R1 (Figure 3), impacted the barrier with appreciable force and is the focus of this analysis.

Figure 3. R1-type synthetic rhombicuboctahedron-shaped rocks.

3.2. *Rockfall Barrier System*

Due to the controlled conditions of the NIOSH rockfall tests, Geobrugg aimed to assess a prototype mobile rockfall barrier system. The proprietary system consisted of concrete-filled tires with embedded vertical steel poles connected by wire mesh (Figure 4). The barrier was assembled on site and positioned at the base of the highwall prior to the rockfall tests (Figure 1). In practice, the purpose of the barrier as erected and positioned would be to protect the LHR from rockfall. All rocks that impacted the barrier were successfully stopped with no discernable damage to the barrier.

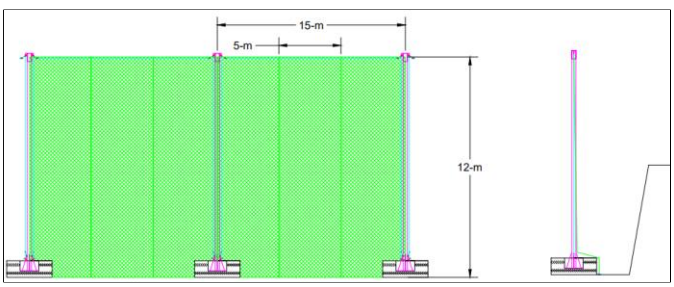

Figure 4. Generic design of the Geobrugg prototype rockfall barrier.

3.3. *R1 Rockfall Kinetics and Kinematics*

Three separate videos of the rockfall tests were collected from two vantage points: a 640x480 resolution thermal video at 30 frames per second and a 4K resolution visual spectrum video at 29.97 frames per second at an overlook location (OV) approximately one km away, and a 4K resolution visual spectrum video at 30 frames per second at a location along the LHR adjacent to the rockfall barrier system. Video stills from OV and LHR are shown in Figure 5a, b, respectively.

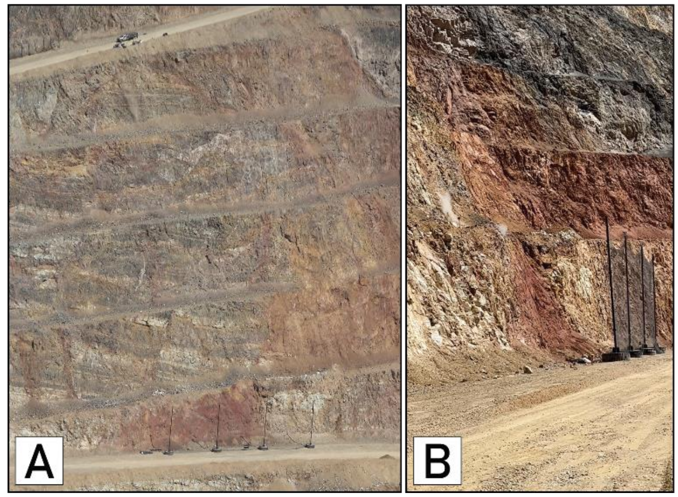

Figure 5. a) video frame from the visual spectrum camera at the OV location. b) video frame from the visual spectrum camera at the LHR location.

Each camera was able to capture the trajectory of the R1 rockfall, with the OV cameras capturing the entirety of the fall nearly parallel to the lateral trajectory of the fall line, and the LHR camera capturing the final bench and impact of the barrier at an oblique view, nearly perpendicular to the fall line. The OV visual spectrum video was used to determine the fall-line of R1, as well as to validate the expected vertical velocities along its trajectory. The photogrammetry-derived point cloud was assessed in CloudCompare (2023) to map the fall-line in 3 dimensions by correlating the R1 impact locations observed in the OV visual spectrum video. This allowed for a more accurate assessment of the horizontal component of velocity based on the lateral distance travelled along its fall. The vertical and horizontal velocity components were then used to calculate the total translational velocity using Eq. 1. Finally, using the estimated velocity profile from Eq. 1 and mass of R1, the total kinetic energy (kJ) profile for R1 was calculated along its trajectory using Eq. 2.

$$V_t = \sqrt{{V_h}^2 + {V_v}^2} \tag{1}$$

$$KE = 0.5mVt^2 \tag{2}$$

Where:

V_t = Total Translational Velocity

V_h = Horizontal Velocity

V_v = Vertical Velocity

KE = Total Kinetic Energy

m = Mass of R1

3.4. *Highwall Bench Configuration*

The point cloud was used to measure catch bench widths (CBW) and bench face angles (BFA) measured along eight profiles parallel to the R1 fall line to provide a broad understanding of how the achieved bench configuration may have influenced the trajectory of R1. The profiles are spaced ~5.5 m within a 40 m wide swath on either side of the R1 fall line. Average CBW and BFA measurements for the eight profiles are presented in Table 2, along with the CBWs and BFAs measured along the R1 fall-line, and the difference between the R1 and average measurements. Table 2 cell colors indicate the range in bench configurations as they relate to rockfall catchment from more favorable (green), to less favorable (red).

Table 2. Measured CBWs and BFAs

	Catch Bench Width (m)			Bench Face Angle (Deg.)		
Bench (m)	Avg.	R1 Fall Line	(R1 - Avg.)	Avg.	R1 Fall Line	(R1 - Avg.)
2254	10.0	10.2	0.1	69.1	69.0	-0.1
2230	10.7	11.3	0.6	65.4	66.0	0.6
2205	9.0	8.0	-1.0	66.8	68.0	1.3
2181	6.9	6.4	-0.5	64.6	63.0	-1.6
2165	-	-	-	63.3	64.0	0.8

3.5. *Rockfall Modelling*

A 2D rockfall model was generated using Rocscience's RocFall2® (2023) software package to mimic the observed R1 trajectory for the purpose of comparison with the R1 test results. A topographic profile for the R1 rockfall was extracted from the 3D point cloud, uploaded to RocFall2®, and simplified to reduce the number of nodes along the profile for reduced processing time. Model parameters for the R1 analysis are provided in Table 3. The initial conditions were estimated from the R1 fall analysis described in section 3.3.

Table 3. Model Parameters for the R1 RocFall2® simulation.

R1 Test Rock	Mass = 172 kg
	Diameter = 46 cm
Initial Horizontal Velocity	4.85 m / s
Initial Rotational Velocity	720 deg / s
Bedrock Highwall Material	Rn = 0.35, Rt = 0.85
	Rolling Friction = 0.15
Talus Highwall Material	Rn = 0.32, Rt = 0.80
	Rolling Friction = 0.30

4. RESULTS

The R1 fall-line topographic profile and estimated R-1 fall trajectory, best-match modeled trajectory, and their respective velocity and total kinetic energy profiles are presented in Figure 6. A satisfactory model fit for the entirety of the R1 trajectory was not achieved, so the best-fit model result was chosen based on the trajectory beneath the 2230 bench level, where the R1 rock bypassed the 2205 bench causing it to accelerate significantly. The calculated velocity and kinetic energy values for R1 and the best-fit model at the moment of impact into the barrier are presented in Table 4.

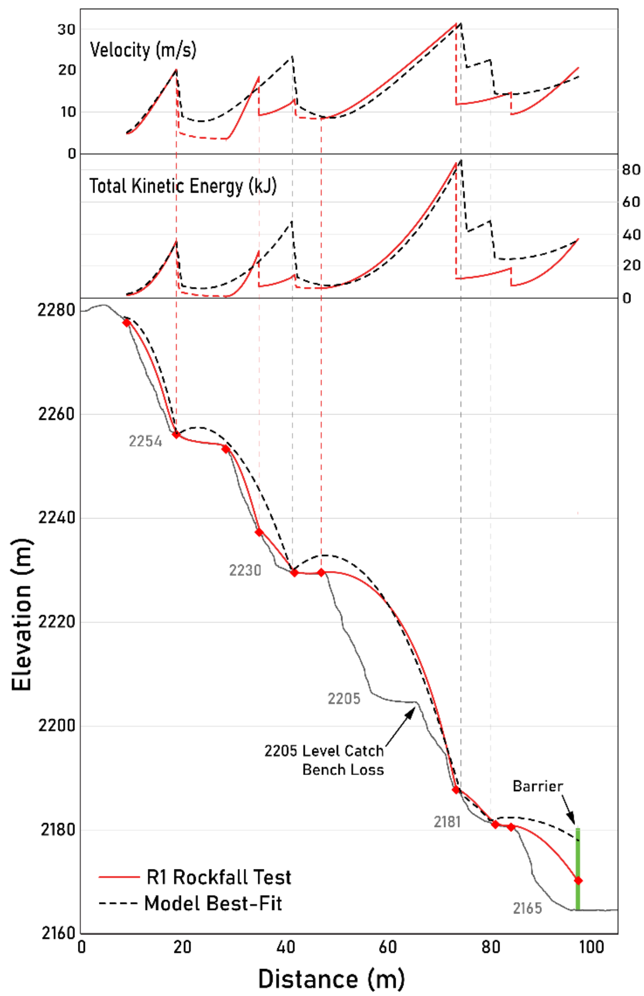

Figure 6. R1 and best-fit model 2D fall trajectories with calculated total kinetic energy and velocity profiles.

Table 4. R1 and best-fit model kinetics upon barrier impact.

	Velocity (m/s)	Total Kinetic Energy (kJ)
R1	20.7	37
Best-Fit Model	18.5	36

5. DISCUSSION

The calculated and best-fit model results for the R1 impact into the barrier prove to be a close match (Table 4), despite the differences in their trajectories prior to impact. The acceleration of R1 upon bypassing the 2205 bench and subsequent fall kinematics below the 2230 bench were the critical factors that resulted in the R1 barrier impact. It appears that about 1-m of catch bench loss observed on the 2205 level (Figure 6, Table 2) resulted in the bypass of the 2205 catch bench. After bypassing the 2205 level, R1 accelerated up to 31 m/s before obliquely striking the bench face above the 2181 level, which increased the horizontal component of its trajectory from an estimated 8.4 m/s to 11.9 m/s, causing it to remain airborne between the 2181 bench and the barrier. Two other test rocks with the same dimension and mass as R1 struck the barrier, however they were slowed therefore prevented from accelerating in the same manner as R1. These blocks made it to the lower haul road and rolled into the barrier with far less force than R1. This suggests that bypassing a single catch bench can propel rocks at dangerously high velocities and trajectories that successive benches are less likely to mitigate. This is especially true when the high vertical velocity achieved from gravitational acceleration is converted to horizontal velocity due to an oblique strike on a bench face, as observed with R1.

Future research may focus on enhancing the model fit with the full R1 trajectory to better calibrate model parameters, specifically the properties of the catch bench material such as the restitution and frictional coefficients. Additionally, more rockfalls from this testing campaign may be analyzed in 2D and 3D to further refine model parameters, and to assess the role of the achieved catch bench configuration in determining the ultimate trajectories and stopping points for rocks of varying mass and dimension. One of the test rocks included an accelerometer that was retrieved after it came to rest on the 2181 catch bench, which may present an opportunity for further calibration of test results.

6. CONCLUSIONS

This study found a close match between the kinetics of empirical and modeled results for a rockfall striking an engineered barrier system in an open pit mine. Importantly, minor catch bench loss resulted in the complete bypass of the 2205 level bench by the R1 test rock, which lead to the acceleration of R1 to high velocities and ultimately a trajectory that would have posed an extreme hazard to the LHR had it not been stopped by the rockfall barrier. Future work may focus on calibrating the model to match the full R1 rockfall kinematics in 2D and 3D, in addition to other rocks of varying mass, dimension, and stopping points that were observed during testing.

7. DISCLAIMERS

The findings and conclusions in this report are those of the author(s) and do not necessarily represent the official position of the National Institute for Occupational Safety and Health, Centers for Disease Control and Prevention. Mention of any company or product does not constitute endorsement by NIOSH, CDC.

REFERENCES

1. Carlà, T., Intrieri, E., Farina, P., & Casagli, N. (2017). A new method to identify impending failure in rock slopes. International Journal of Rock Mechanics and Mining Sciences, 93, 76–81. https://doi.org/10.1016/j.ijrmms.2017.01.015
2. CloudCompare. (2023). CloudCompare (Version 2.13. Beta) [GPL Software].CloudCompare. http://www.cloudcompare.org/
3. Farina, P., Coli, N., Yön, R., Eken, G., & Ketizmen, H. (2013). Efficient real time stability monitoring of mine walls: The çöllolar mine case study. 23rd International Mining Congress and Exhibition of Turkey, IMCET 2013, 1, 111–117.
4. Gerber. (2001). Guideline for the Approval of Rockfall Protection Kits [Rock Mechanics—Rock Falls]—Geotechpedia. https://geotechpedia.com/Publication/Show/1371/guideline-for-the-approval-of-rockfall-protection-kits
5. Jaboyedoff, M., Dudt, J.-P., & Labiouse, V. (2005). An attempt to refine rockfall hazard zoning based on the kinetic energy, frequency and fragmentation degree. Natural Hazards and Earth System Sciences, 5. https://doi.org/10.5194/nhess-5-621-2005
6. Mentani, A., Govoni, L., Gottardi, G., Lambert, S., Bourrier, F., & Toe, D. (2016). A New Approach to Evaluate the Effectiveness of Rockfall Barriers. Procedia Engineering, 158, 398–403. https://doi.org/10.1016/j.proeng.2016.08.462
7. NIOSH. (2022). Mining Project: Highwall Safety: Rockfall Catchment Design and Slope Performance Monitoring at Surface Mines and Quarries. Retrieved from: https://www.cdc.gov/niosh/mining/researchprogram/projects/project_highwallsafety.html
8. NIOSH. (2023). Mining Contract: Development of Automated Rockfall Detection via Thermal Video Cameras in Open Pit Mines. Contract number 75D30122C14875. Retrieved from: https://www.cdc.gov/niosh/mining/researchprogram/contracts/contract_75D30122C14875.html
9. Rocscience. (2023). RocFall2 (Version 8.024) [Computer Software]. Rocscience. https://www.rocscience.com/software/rocfall

10. Sanchez, M. A., & Caviezel, A. (2020). Full-scale testing of rockfall nets in real terrain. Results of tests at Chant Sura: 13th September and 4th October, 2019. https://www.dora.lib4ri.ch/wsl/islandora/object/wsl%3A24633/

11. Spadari, M., Giacomini, A., Buzzi, O., & Hambleton, J. P. (2012). Prediction of the Bullet Effect for Rockfall Barriers: A Scaling Approach. Rock Mechanics and Rock Engineering, 45(2), Article 2. https://doi.org/10.1007/s00603-011-0203-0

12. Warren, S., Bourgeois, J., Sweet, D., S., Brackebusch, A., Stopka, C., & Armstrong, J. (2022, November 8). Revisiting Rockfall Catch Bench Design Criteria: Initial Rockfall Testing Results from the Golden Chest Mine, ID.

13. Williams, C., Morkeh, J., Dorfschmidt, K., Poon, C., Matlashewski, P., & Carvalho, J. (2020). Innovative Rockfall Solutions Based on Calibration and Field Testing. Mining, Metallurgy & Exploration, 37(1), 101–116. https://doi.org/10.1007/s42461-019-0092-4